Frequency selective surfaces with nanoparticles unit cell

Poon, Nga Hung; Yan, Yan; Zhou, Li; Wang, Desong; Chan, Chi-Hou; Roy, Vellaisamy A.L.

Published in:
Micromachines

Published: 01/01/2015

Document Version:
Final Published version, also known as Publisher's PDF, Publisher's Final version or Version of Record

Published version (DOI):
10.3390/mi6101421

Publication details:
Poon, N. H., Yan, Y., Zhou, L., Wang, D., Chan, C.-H., & Roy, V. A. L. (2015). Frequency selective surfaces with nanoparticles unit cell. *Micromachines*, *6*(10), 1421-1426. https://doi.org/10.3390/mi6101421

micromachines

MDPI

Communication

Frequency Selective Surfaces with Nanoparticles Unit Cell†

Nga Hung Poon [1], Yan Yan [1], Li Zhou [1], Desong Wang [2,3], Chi-Hou Chan [2,3] and Vellaisamy A. L. Roy [1,2,*]

Received: 20 July 2015 ; Accepted: 14 September 2015 ; Published: 25 September 2015
Academic Editors: Wen Jung Li and Ting-Hsuan Chen

[1] Department of Physics and Materials Science, City University of Hong Kong, Tat Chee Avenue, Kowloon Tong, Hong Kong, China; poonngahung2005@gmail.com (N.H.P.); yyan26-c@my.cityu.edu.hk (Y.Y.); lizhou-c@my.cityu.edu.hk (L.Z.)
[2] State Key Laboratory for Millimeter Waves, City University of Hong Kong, Tat Chee Avenue, Kowloon Tong, Hong Kong, China; dswang2@cityu.edu.hk (D.W.); eechic@cityu.edu.hk (C.-H.C.)
[3] Department of Electronic Engineering, City University of Hong Kong, Tat Chee Avenue, Kowloon Tong, Hong Kong, China
* Correspondence: val.roy@cityu.edu.hk; Tel.: +852-3442-2729
† This paper is an extended version of our paper published in the 10th Annual IEEE International Conference on Nano/Micro Engineered and Molecular Systems (IEEE NEMS 2015), Xi'an, China, 7–11 April 2015.

Abstract: The frequency selective surface (FSS) is a periodic structure with filtering performance for optical and microwave signals. The general periodic arrays made with patterned metallic elements can act as an aperture or patch on a substrate. In this work, two kinds of materials were used to produce unit cells with various patterns. Gold nanoparticles of 25 nm diameter were used to form periodic monolayer arrays by a confined photocatalytic oxidation-based surface modification method. As the other material, silver gel was used to create multiple layers of silver. Due to the ultra-thin nature of the self-assembled gold nanoparticle monolayer, it is very easy to penetrate the FSS with terahertz radiation. However, the isolated silver islands made from silver gel form thicker multiple layers and contribute to much higher reflectance. This work demonstrated that multiple silver layers are more suitable than gold nanoparticles for use in the fabrication of FSS structures.

Keywords: frequency selective surface (FSS); amine functionalization; time-domain spectroscopy (TDS) system

1. Introduction

Frequency selective surfaces (FSSs) have been intensively investigated for more than four decades due to their widespread applications as spatial microwave and optical filters [1–4]. FSSs are usually constructed from periodically arranged metallic patches of arbitrary geometries or their complementary structures, which have aperture elements similar to patches within metallic screens [5]. These surfaces can exhibit total reflection or transmission in the neighborhood of the element resonances. The proper choice of constituent elements for the array is the most important step in the design of a desired FSS. The overall frequency response of the structure is generally determined by the element type, geometry, substrate parameters, and inter-element spacing. Many methods have been devised to improve the performance of FSSs, such as the dielectric loading FSS, biplanar FSS, complementary FSS, close-coupled FSS, and reconfigurable FSS [6–9]. However, the shapes and configurations that can be chosen for the FSS elements are limited. An FSS is usually made of metallic periodic array, such as aluminum, gold (Au), and copper [10,11]. In recent years, nanoparticles

have been the center of attention of researchers in many fields due to the immense changes that occur in the physical and chemical properties of a material during the transition process from bulk materials to nanoparticles [12,13]. Nanoparticles have also received considerable attention due to their unique and novel magnetic, optical, electronic, and catalytic properties. They have been widely used in areas such as biomedicine, catalysis, fuel cells, magnetic data storage, and solar cells [14–20]. In this work, to replace patterned arrays made of general metallic materials, a self-assembled gold nanoparticle (Au NP) monolayer and silver isolated islands made of conductive silver gel are used to form FSS structures and the performance of the two structures at terahertz frequency is measured. The fabrication process of the FSS structure is a low temperature process. In addition, it is a low-cost process suitable for large-area fabrication and compatible for roll-to-roll fabrication.

2. Experimental Section

2.1. Material

Polyethylene terephthalate (PET) of 160 μm thickness was used as the flexible substrate of the FSS. Material ammonium persulfate, (3-Aminopropyl)triethoxysilane (APTES), Au NPs, and ethanol were used for surface modification on the PET substrate. Silver plate gel was required for the silver coating on the PET film.

2.2. Chromium Masks

To form the patterns of Au NPs on the PET substrates by confined photocatalytic oxidation (CPO)-based surface modification, chromium masks with hexagonal and circular patterns were fabricated, with each mask containing 900 (30 × 30) unit cells [21]. The diameter of each unit cell pattern was designed in accordance with software simulation results of the reflection characterization of terahertz FSS.

2.3. Synthesis of 25 nm Gold Nanoparticles

A 20 mL amount of 2.5×10^{-4} M gold(III) chloride trihydrate ($HAuCl_4 \cdot 3H_2O$) (Sigma-Aldrich, St. Louis, MI, USA, >99%) solution was heated to boiling, and 1 mL of 25 mM sodium citrate (Sigma-Aldrich, ⩾98%) was injected rapidly into the solution under vigorous stirring. After boiling for 30 min, the solution was left to cool to room temperature. The solution was washed twice with de-ionized water (DI water) to remove the redundant sodium citrate, first by centrifugation and then by re-dispersal into the DI water.

2.4. Sample Fabrication and Characterization

Before surface modification of the flexible PET films, the substrates were cleaned by DI water to remove the impurities and contaminants on the surface. Then, a persulfate salt aqueous solution (30 wt %) was dropped on the PET films with a patterned quartz glass mask covering the surface. The sandwich structure was exposed under ultraviolet (UV) light for 20 min. After the surface reaction on the PET films was complete, the substrates were cleaned using ultrapure water to remove any residual reaction solution. The modified PET films were again placed in ultrapure water to remove residual reaction solution on the surface. Then, the modified PET films were placed in ultrapure water for 6 h to generate rich C–OH groups. Thereafter, the substrates with rich OH groups were immersed in APTES ethanol solution (0.1 wt %) for 2 h to form a high density of NH_2 groups on the reacted surface. The modified films were then placed in the Au NPs solution for 10 h so that the Au NPs could tightly connect with the modified PET substrates by chemical bonding. Finally, the substrates with the patterned Au NP monolayer were simply cleaned with DI water and placed on a hot plate at 100 °C for 30 min. For comparison against the patterned Au NP monolayer surface, a patterned silver film coating made from conductive silver gel was applied on the PET. The patterned structure was fabricated under an optical microscope by stamping silver gel onto each unit cell by hand. The

size of the nanoparticles was scanned by transmission electron microscope (JSM-2100 F, JEOL Ltd., Tokyo, Japan) and the film of gold nanoparticles on the PET substrate was characterized by scanning electron microscope (JSM-6335F, JEOL Ltd.). The surface roughness of the films was measured by a Veeco Multimode V atomic force microscope (AFM).

The UV light for the CPO reaction was provided by an ultra-high-intensity UV spot lamp (50,000 $\mu W/cm^2$) with a wavelength (λ) of 365 nm. A time-domain spectroscopy (TDS) system (EKSPLA, Vilnius, Lithuania) was used to evaluate the frequency characteristics of the fabricated FSS samples. The THz spectrometer has a pulse duration of less than 90 fs and a spectral range of 0.1 to 3.5 THz. Through time-domain measurements and subsequent Fourier transforms of the temporal data, scattering (S) parameters of the THz FSS could be obtained.

3. Results and Discussion

3.1. Surface Modification

The process of applying a CPO-based Au NP monolayer surface pattern onto flexible PET substrate is depicted in Figure 1. The CPO treatment was used on PET film surfaces, followed by a hydrolysis process, to convert the alkyl C–H groups on the PET surface to C–OH groups.

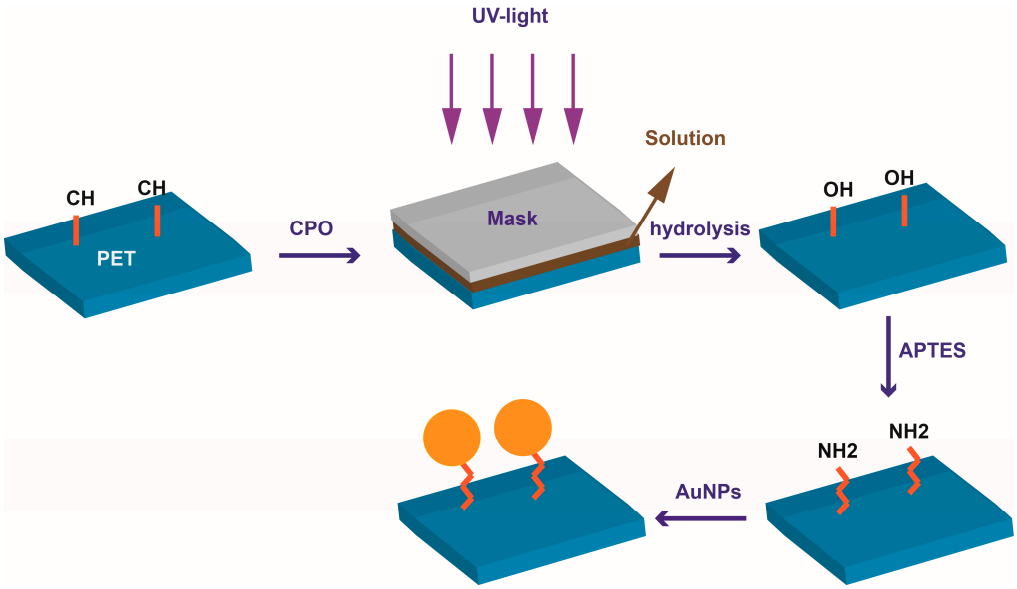

Figure 1. Schematic diagram depicting application of the confined photocatalytic oxidation (CPO) based self-assembled gold nanoparticle (Au NP) monolayer surface pattern on flexible polyethylene terephthalate (PET) substrate.

Subsequently, silanization was carried out on the flexible substrates. With the rich OH groups as reaction sites, a high density of NH_2 groups could be successfully implanted on the treated PET surface. Finally, the Au NPs were tightly connected with the modified PET substrates full of NH_2 groups by chemical bonding, and the patterned Au NP monolayer film was formed.

Figure 2 shows optical microscope images of FSSs with the patterned gold monolayer. The patterns of hexagonal and circular cells are uniform and periodical, which indicates that the CPO-based surface modification is quite suitable for use in forming variously patterned shapes with an Au NP monolayer. The periodically arranged patterned film is necessary for an FSS structure to exhibit total reflection or transmission. Figure 3a shows the TEM image of gold nanoparticles, and we can find that the size of nanoparticles is around 25 nm and relatively uniform. Figure 3b displays the SEM image of the gold nanoparticle monolayer on the PET substrate. We can observe that gold

nanoparticles with high density are attached on the top of the PET film. The root-mean-square (RMS) roughness of the nanoparticle monolayer on the PET surface is about 11.5 nm.

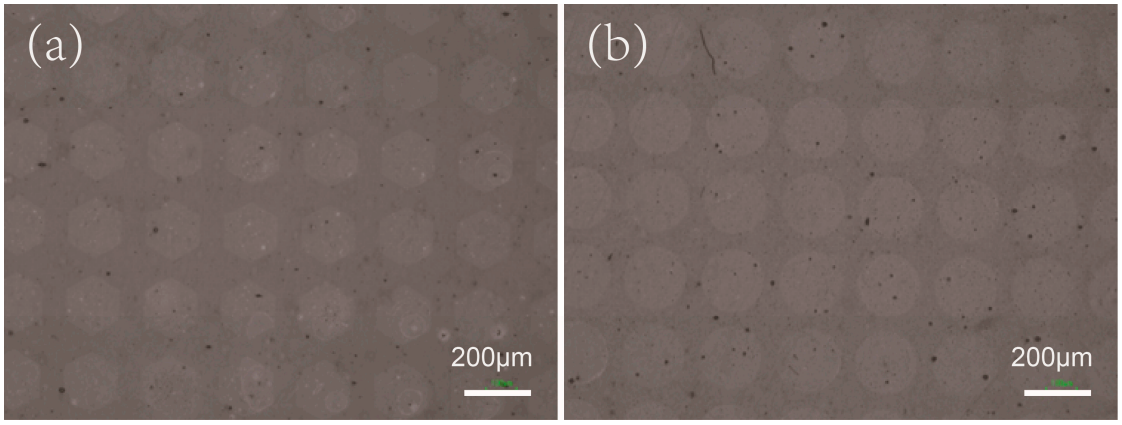

Figure 2. Optical microscope images of the frequency selective surface (FSS) with the patterned hexagonal (**a**) or circular (**b**) Au NP monolayer.

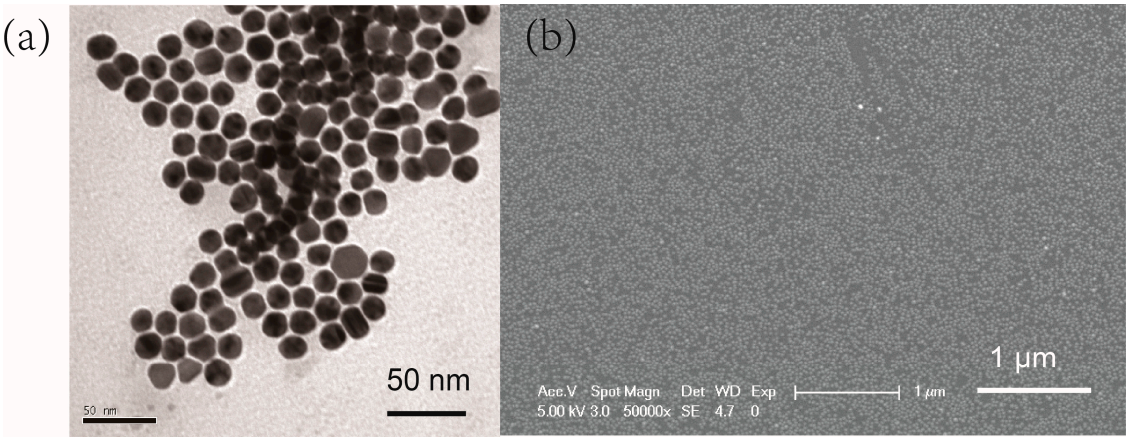

Figure 3. (**a**) Transmission Electron Microscope image of gold nanoparticle and (**b**) Scanning Electron Microscope image of gold nanoparticle monolayer on the PET substrate.

3.2. TDS Results

The TDS measurement and simulation results of FSSs with hexagonal and circular Au NP monolayers are shown in Figure 4. High-Frequency Structure Simulator (HFSS from ANSYS, Inc., Canonsburg, PA, USA) was chosen as the simulation software. For HFSS simulations, the Au NP monolayer is modeled with gold patches of zero thickness with a conductivity of 4.1×10^{-7} s/m. The exact thickness of the gold monolayer of 25 nm could not be modeled by HFSS as the aspect ratio of the elements would be too large, considering that the unit-cell spacing is 250 μm in both transverse directions. The PET substrate has a thickness of 160 μm with a dielectric constant of 2.95 and loss tangent of 0.07. The simulated hexagonal- and circular-patch FSSs show band-stop frequency responses with center frequencies of 0.81 and 0.79 THz, respectively. The simulated maximum reflections in the desired frequency range are more than 95% for the two FSSs. It is of note that the noise waves are close to the frequency band of interest for the two FSS structures and, thus, degrade the overall filtering performance. This fact results from the pattern shapes used, but that is not the focus of this study. Both of the fabricated FSS patterns show a reflectance of only 20%, which is the same as that of the pure PET substrates. However, this does not agree with the results of the simulated FSSs with zero-thickness gold patches. This finding was attributed to the small nanoparticles whose

diameter and thickness are similar to the surface skin depth and whose reflectance is much less than the wavelength of the THz FSSs. The skin depth at THz range is larger than the thickness of the nanoparticles (25 nm). The calculated skin depth at 800 GHz is around 80 nm, considering the bulk conductivity of the gold. Therefore, the skin effect considerably weakens the reflectance at the THz frequency.

To further investigate the FSS structures, two hexagonal- and circular-patch FSSs were fabricated again by manually replacing the nanoparticle patterns with silver patterns. The TDS measurement results are shown in Figure 5. The measured maximum reflectances are about 50% at 0.55 THz and 40% at 0.35 THz for the hexagonal- and circular-patch FSSs. The maximum reflectances of the FSSs with the silver patterns are larger than those of the PET substrates (25% at around 0.75 THz), thereby indicating that the silver patterns improved the reflective properties of the FSSs. Therefore, it can be concluded that one can realize high-performance THz FSSs by using either thick or multilayer NPs.

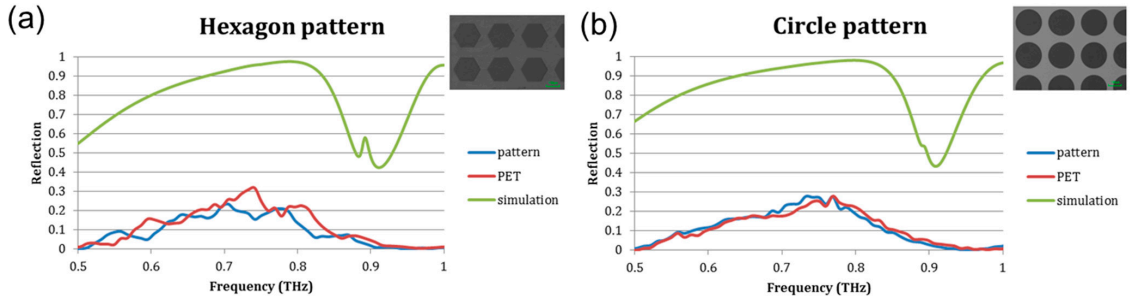

Figure 4. Time-domain spectroscopy (TDS) measurement and simulation results of FSSs made with an Au NP monolayer with hexagonal (**a**) and circular (**b**) patterns.

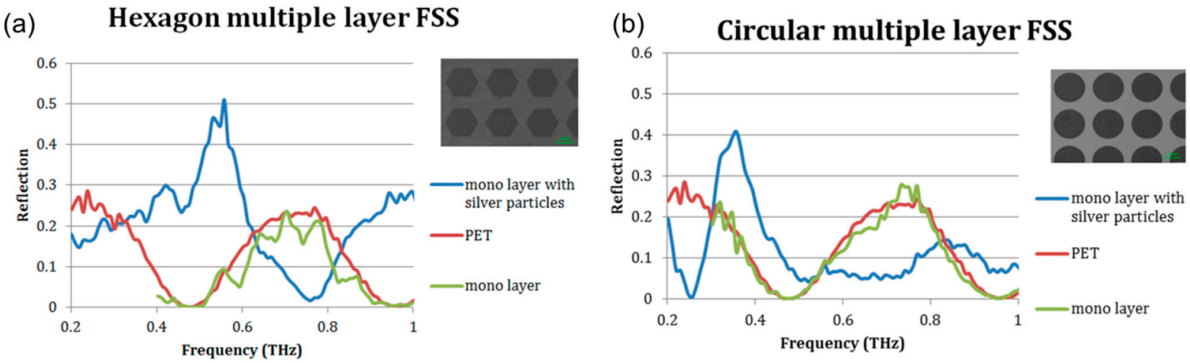

Figure 5. TDS measurements of FSSs made of silver-isolated islands with hexagonal (**a**) and circular (**b**) shapes.

4. Conclusions

In conclusion, we used two kinds of metallic materials to fabricate FSS structures. The FSS structure made with the self-assembled 25 nm Au NPs as the metallic material of the ultrathin monolayer was very easily penetrated by THz radiation. It is therefore not suitable for use in the fabrication of THz FSS structures. The silver-isolated islands made of silver gel, which possess the same shape and size of the FSS structure with circular or hexagonal arrays, could form multiple and thicker layers, and showed much higher reflectance. This indicates that the multiple silver layers are much more suitable than the Au NP monolayer for use in the fabrication of FSS structures.

Acknowledgments: We acknowledge grants from City University of Hong Kong's Grant Project No. 7004198 and 9678064.

Author Contributions: Nga Hung Poon performed the experiments and wrote the paper. Yan Yan assisted with surface modification on polymeric surface. Li Zhou assisted with the Au NP fabrication. Desong Wang assisted with TDS measurements and simulation. Vellaisamy A. L. Roy and Chi-Hou Chan supervised the project and finalized the manuscript.

Conflicts of Interest: The authors declare no conflict of interest.

References

1. O'Nians, F.; Matson, J. Antenna Feed System Utilizing Polarization Independent Frequency Selective Intermediate Reflector. U.S. Patent 3,231,892, 25 January 1966.
2. Ott, R.; Kouyoumjian, R.; Peters, L., Jr. Scattering by a two dimensional periodic array of narrow plates. *Radio Sci.* **1967**, *2*, 1347–1359.
3. Munk, B.; Kouyoumjian, R.; Peters, L., Jr. Reflection properties of periodic surfaces of loaded dipoles. *IEEE Trans. Antennas Propag.* **1971**, *19*, 612–617. [CrossRef]
4. Mittra, R.; Chan, C.H.; Cwik, T. Techniques for analyzing frequency selective surfaces—A review. *Proc. IEEE* **1988**, *76*, 1593–1615. [CrossRef]
5. Sarabandi, K.; Behdad, N. Frequency Selective Surface with Miniaturized Elements. *IEEE Trans. Antennas Propag.* **2007**, *55*, 1239–1245. [CrossRef]
6. Luebbers, R.; Munk, J.B.A. Some effects of dielectric loading on periodic slot arrays. *IEEE Trans. Antennas Propag.* **1978**, *26*, 536–542. [CrossRef]
7. Vardaxoglou, J.C.; Lockyer, D.S. Modified FSS response from two sided and closely coupled arrays. *Electron. Lett.* **1994**, *30*, 1818–1819. [CrossRef]
8. Lockyer, D.S.; Moore, C.M.; Seager, R.; Simpkin, R.; Vardaxoglou, J.C. Coupled dipole arrays as reconfigurable frequency selective surfaces. *Electron. Lett.* **1994**, *30*, 1258–1259. [CrossRef]
9. Lockyerd, D.S.; Vardaxoglou, J.C. Reconfigurable FSS from two layers of slotted dipole arrays. *Electron. Lett.* **1996**, *32*, 512–513. [CrossRef]
10. Wu, T.K. *Frequency Selective Surface and Grid Array*; Wiley: New York, NY, USA, 1995.
11. Munk, B.A. *Frequency Selective Surfaces: Theory and Design*; Wiley: New York, NY, USA, 2000.
12. Chaudhuri, R.G.; Paria, S. Core/Shell Nanoparticles: Classes, Properties, Synthesis Mechanisms, Characterization, and Applications. *Chem. Rev.* **2012**, *112*, 2373–2433. [CrossRef]
13. Thanh, N.T.K.; Maclean, N.; Mahiddine, S. Mechanisms of Nucleation and Growth of Nanoparticles in Solution. *Chem. Rev.* **2014**, *114*, 7610–7630. [CrossRef] [PubMed]
14. Thanh, N.T.K. *Magnetic Nanoparticles: From Fabrication to Clinical Applications*; CRC Press/Taylor and Francis: Boca Raton, FL, USA; London, UK, 2012.
15. Pankhurst, Q.A.; Thanh, N.T.K.; Jones, S.K.; Dobson, J. Progress in applications of magnetic nanoparticles in biomedicine. *J. Phys. D App. Phys.* **2009**, *42*, 224001. [CrossRef]
16. Narayanan, R.; El-Sayed, M.A. Catalysis with Transition Metal Nanoparticles in Colloidal Solution: Nanoparticle Shape Dependence and Stability. *J. Phys. Chem. B* **2005**, *109*, 12663–12676. [CrossRef] [PubMed]
17. Astruc, D.; Lu, F.; Aranzaes, J.R. Nanoparticles as recyclable catalysts: The frontier between homogeneous and heterogeneous catalysis. *Angew. Chem. Int. Ed.* **2005**, *44*, 7852–7872. [CrossRef] [PubMed]
18. Bönnemann, H.; Richards, R. Nanoscopic Metal Particles-Synthetic Methods and Potential Applications. *Eur. J. Inorg. Chem.* **2001**, *2001*, 2455–2480. [CrossRef]
19. Hyeon, T. Chemical synthesis of magnetic nanoparticles. *Chem. Commun.* **2003**, *2003*, 927–934. [CrossRef]
20. Atwater, H.A.; Polman, A. Plasmonics for improved photovoltaic devices. *Nat. Mater.* **2010**, *9*, 205–213. [CrossRef] [PubMed]
21. Yang, P.; Yang, W. Hydroxylation of organic polymer surface: Method and application. *ACS Appl. Mater. Interfaces* **2014**, *6*, 3759–3770. [CrossRef] [PubMed]